

# Quantum-degenerate mixture of fermionic lithium and bosonic rubidium gases

C. Silber, S. Günther, C. Marzok, B. Deh, Ph.W. Courteille, and C. Zimmermann  
*Physikalisches Institut, Eberhard-Karls-Universität Tübingen,  
 Auf der Morgenstelle 14, D-72076 Tübingen, Germany*

(Dated: March 21, 2019)

We report on the observation of sympathetic cooling of a cloud of fermionic  ${}^6\text{Li}$  atoms which are thermally coupled to evaporatively cooled bosonic  ${}^{87}\text{Rb}$ . Temperatures below the Fermi temperature have been reached. From measurements of the thermalization velocity we estimate the interspecies  $s$ -wave triplet scattering length  $|a_s| = 17_{-6}^{+9} a_B$ . We found that the presence of residual rubidium atoms in the  $|2, 1\rangle$  and the  $|1, -1\rangle$  Zeeman substates gives rise to important losses due to inelastic collisions.

PACS numbers: 05.30.Fk, 05.30.Jp, 32.80.Pj, 67.60.-g

The recent realization of degenerate gases of homonuclear diatomic molecules is an important achievement for the physics of ultracold dilute quantum gases [1, 2]. The key to this spectacular success was the use of Feshbach resonances which allow for an adiabatic transformation from free pairs to molecules in the least bound state close to the dissociation energy [3]. The large internal energy makes the gas unstable against collisions between the molecules, which transform the energy into kinetic energy of the collision partners [4]. The very long lifetimes of up to several 10 s observed for dimers made of fermionic  ${}^6\text{Li}$  [2] are explained by the fact that the atoms are only loosely bound with a binding energy of 1  $\mu\text{K}$  such that the bound atoms still behave very much like individual atoms [5]. Collisions are thus suppressed due to Pauli-blocking. Fermionic lithium is now a very promising candidate for exploring the cross-over regime between the Bardeen-Cooper-Schrieffer (BCS) model for superconductivity based on Cooper pairs and the regime of a Bose-Einstein condensate of composite bosons [6]. If magnetically trapped in a highly anisotropic magnetic trap and prepared in the degenerate regime, such a molecular Fermi gas would be a very clean realization of a one-dimensional Luttinger liquid [7].

In contrast to homonuclear dimers molecules made of two different atomic species exhibit a permanent electric dipole moment. The  $\text{LiRb}$  dimer has a very large permanent electric dipole moment of 4.13 Debye [8]. The intermolecular interaction in such a heteronuclear gas has a pronounced long-range character, which fundamentally alters its behavior at low temperatures [9] and brings global properties of the gas into play. E.g. the geometric shape of the cloud for instance will influence the total interaction energy and thus the stability of the gas [10].

A possible approach to generate a polar molecular gas would use a Feshbach resonance in close analogy to the homonuclear experiments [1, 2]. Only recently first heteronuclear Feshbach resonances have been observed [11]. Heteronuclear molecular gases are expected to be relatively stable against collisions if one of the two atoms is a fermion [5]. For such a weakly bound molecule Pauli-blocking is at least partially effective. As an alternative to Feshbach resonances, photoassociation is used to

transform atomic pairs into molecules. Photoassociation has been extensively investigated for the homonuclear case [12] and there are already examples of successful heteronuclear photoassociation [13, 14, 15]. The advantage of photoassociation is the possibility to form molecules also in deeper lying bound states, where the internuclear distance is drastically reduced and the molecules behave more like composite particles with a well defined quantum statistics. Furthermore, the dipole moment is largest for deeply bound states.

Besides their importance for generating molecular gases, mixtures have remarkable physical properties which cannot be observed in pure quantum gases. Among them are phase separation effects [16] and collective excitations due to mutual mean field interaction between the mixed gases [17]. The interaction between fermions can be strongly modified in the presence of a bosonic background gas [18]: Similar to phonon-induced formation of Cooper pairs in superconductors, it is expected that an atomic Fermi gas can be driven into a BCS transition by mediation of the Bose gas.

The practical reason to work with mixtures is, that thermal coupling to a different species is the key to cooling a Fermi gas [19, 20]. Various mixtures of bosonic and fermionic alkalis are currently under investigation. In this work we report on the first studies with mixtures of fermionic  ${}^6\text{Li}$  with  ${}^{87}\text{Rb}$ . We demonstrate that sympathetic cooling works down to the regime of Fermi degeneracy, provided special care is taken to ensure the purity of the Rb cloud. Indeed, the presence of  $|2, 1\rangle$  or  $|1, -1\rangle$  atoms leads to large inelastic Li losses at high densities, and their removal from the trap is a precondition to achieve Fermi degeneracy. Furthermore, we measure the interspecies thermalization speed and derive a value for the scattering length for heteronuclear collisions.

The scheme of our experiment is as follows: We simultaneously load  ${}^{87}\text{Rb}$  atoms from a dispenser and  ${}^6\text{Li}$  atoms from a Zeeman slower [13] into superposed standard magneto-optical traps (MOT). From here the atoms are transferred into a magnetic quadrupole potential operated with the same coils as the MOT. With a spin-polarizing light pulse the Li and Rb atoms are transferred to the hyperfine states  $| \frac{3}{2}, \frac{3}{2} \rangle$  and  $|2, 2\rangle$ , respectively. The

potential is then compressed and, with an arrangement inspired by Ref. [21], the atoms are transferred via a second into a third quadrupole trap [cf. Fig. 1(a)]. Via two pairs of 0.9 mm thick wires running parallel to the symmetry axis of the third quadrupole trap a Ioffe-Pritchard type potential is created [22]. For typical operating conditions the potential energy increases linearly with the radial distance from the center and quadratically with the axial distance. Only very close to the center, i.e. for temperatures of the atoms in the  $\mu\text{K}$  range, the trap is harmonic.

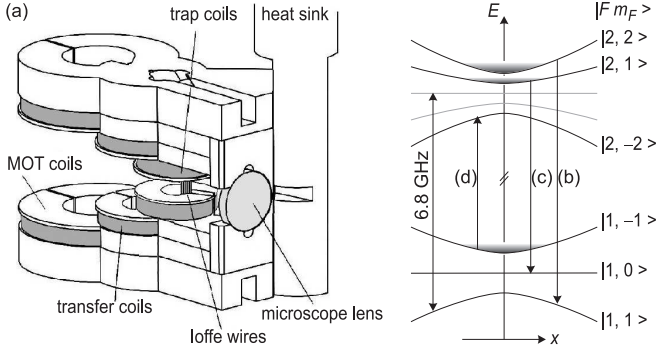


FIG. 1: (a) Setup for simultaneous trapping of lithium and rubidium. The scale of the drawing is 1:5. All parts are located inside the vacuum chamber. After optical cooling between the MOT-coils, both clouds are transferred into a Ioffe-Pritchard trap by adiabatic transfer with three pairs of coils. In the trap the atoms are optically accessible from all six directions. Both clouds can be monitored simultaneously by absorption imaging. The right figure shows the scheme of the microwave transitions used (b) for evaporating the Rb cloud in the  $|2, 2\rangle$  state, (c) for removing atoms from the  $|2, 1\rangle$  state and (d) for removing atoms from the  $|1, -1\rangle$  state.

The Rb cloud is cooled by forced evaporation: A microwave frequency resonantly tuned to the ground state hyperfine structure couples the trapped Zeeman state  $|2, 2\rangle$  and the untrapped  $|1, 1\rangle$ , as shown in figure 1(b). After 15 s of down-ramping the microwave, we reach the threshold to quantum degeneracy at  $T_c = 620 \text{ nK}$  with about  $N_{87} = 1.2 \times 10^6$  atoms. For the sake of definiteness, here and in the following we assign the subscripts 6 to lithium and 87 to rubidium quantities. Typical trap frequencies at the end of the evaporation ramp are  $\omega_x \approx \omega_y \simeq 2\pi \times 206 \text{ Hz}$  and  $\omega_z \simeq 2\pi \times 50.1 \text{ Hz}$ , obtained at a bias field of 3.5 G. Cooling down further yields almost pure condensates of  $5 \times 10^5$  Rb atoms. The microwave is parked at 100 kHz above the potential minimum to prevent heating due to glancing collision with the background gas, whose pressure is a few times  $10^{-11} \text{ mbar}$ . The condensate lifetime is about 1 s.

At the beginning of the evaporation ramp the Li cloud consists of about  $2 \times 10^7$  atoms. In the absence of Rb atoms the lifetime of the Li cloud is about 170 s. As a result of the evaporative cooling of the Rb cloud, the Li cloud is cooled sympathetically provided the evaporation ramp is slow enough, i.e. in practice 25 s. We found that,

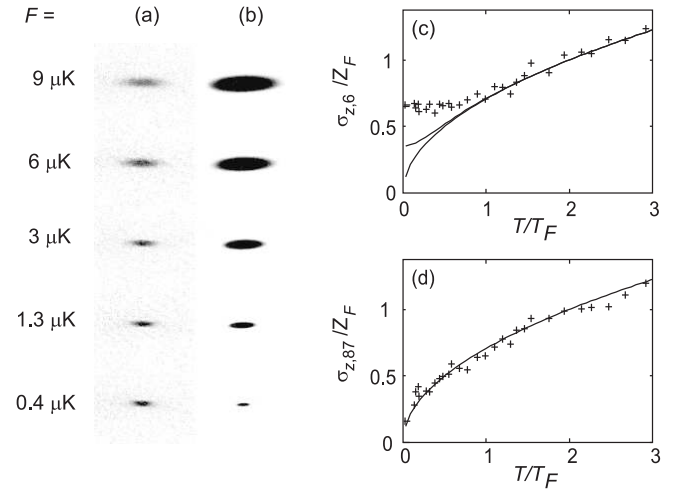


FIG. 2: Simultaneous *in-situ* absorption pictures of the Li Fermi-gas (a) and the Rb Bose-condensate (b) taken at different stages of the evaporation process. Temperatures are determined from 15 ms time-of-flight absorption images of the Rb cloud. The axial (horizontal) size of the Li cloud is clearly limited to values  $2\sigma_{z,6} \gtrsim 80 \mu\text{m}$ . In contrast, the Rb condensate shrinks at lower temperatures. From such absorption images we determine the temperature dependence of the axial *rms*-radii of (c) the trapped Li cloud and (d) the trapped Rb cloud. The theoretical curves show the temperature dependence expected for a gas of classical particles (dotted lines) and for a gas of fermions (solid lines) with  $N_6 = 2 \times 10^5$  particles. The Rb and the Li data have been scaled with a common factor to rule out uncertainties in the magnification of the imaging system.

if the ramp is too fast, the Li cloud thermally decouples from the Rb cloud. This behavior indicates a small interspecies collision rate. We also noticed dramatic losses for the Li cloud that will be discussed below. At the end of the evaporation ramp we let the clouds equilibrate for 1 s before imaging them inside the trap [cf. Fig. 2(a,b)].

The Fermi temperature is reached with typically  $N_6 = 2 \times 10^5$  Li atoms *above* the critical temperature for Bose-Einstein condensation:  $T_F = T_c \sqrt{87/6} [6\zeta(3)N_6/N_{87}]^{1/3} \simeq 2.4 \mu\text{K}$ , where  $\zeta(3) = 1.202$ . This ensures a good spatial overlap between the clouds, which is important to avoid spatial separation in the gravity field. For our conditions we expect a relative gravitational sag,  $\Delta y = 6 \mu\text{m}$ , smaller than the classical *rms*-radii of the clouds,  $\sigma_{r,6} = \sigma_{r,87} \simeq 15 \mu\text{m}$ . When the Rb cloud is cooled to temperatures below  $T_F$ , we observe that the axial radius of the trapped Li cloud reaches a lower bound at values below the *rms*-Fermi radius,  $\sigma_{z,6} < Z_F/\sqrt{2} = \sqrt{k_B T_F/m_{87} \omega_z^2} \simeq 62 \mu\text{m}$ , but above the theoretical prediction,  $\sigma_{z,6} > Z_F/\sqrt{8}$  [cf. Fig. 2(c,d)]. This behavior may be explained by a joined impact of fermionic quantum statistics and a deceleration of sympathetic cooling as the number of Rb atoms decreases through forced evaporation. The weakening of the thermal coupling, which seems to have played a role in previ-

ous experiments [20, 23], is more pronounced in our case by the slow Li-Rb cross species thermalization rate.

In the presence of Rb atoms we observe a steady decrease in the Li atom number. The decrease, which is faster at high Rb densities, completely dominates the time scales, and if no measure is taken to slow it down, the Li cloud disappears well before the Fermi temperature is reached. These Li trap losses are induced on one hand by  $|1, -1\rangle$  Rb atoms, which remain in the trap because the initial spin polarizing pulse fails to transfer all atoms into the fully stretched state. On the other hand, we observe that  $|2, 1\rangle$  Rb atoms are produced out of the  $|2, 2\rangle$  cloud on a continuous basis. This spin relaxation is probably due to Majorana spin flip transitions carried out by fast atoms crossing the potential minimum and to inelastic spin exchange collisions induced by dipolar interactions [24]. The  $|2, 1\rangle$  atoms then inelastically collide with  $|\frac{3}{2}, \frac{3}{2}\rangle$  Li atoms to give rise to one of the following product combinations:  $|2, 2\rangle + |\frac{3}{2}, \frac{1}{2}\rangle$  or  $|2, 2\rangle + |\frac{1}{2}, \frac{1}{2}\rangle + \hbar\omega_{6,\text{hfs}}$  or  $|1, 1\rangle + |\frac{3}{2}, \frac{3}{2}\rangle + \hbar\omega_{87,\text{hfs}}$ , since the total magnetic quantum number  $m_F$  is good at all internuclear distances [17]. Losses for dense clouds induced by populated wrong hyperfine states have been observed earlier [23].

Note that the microwave frequency used by us for evaporation is selective to the  $|2, 2\rangle$  state, so that  $|2, 1\rangle$  atoms remain and accumulate in the trap. This is in contrast to experiments using a radiofrequency, where hot  $|2, 1\rangle$  atoms are evaporated from the trap together with hot  $|2, 2\rangle$  atoms. To eliminate the harmful impact of the  $|2, 1\rangle$  atoms, we selectively remove them from the trap. This is done by applying a magnetic field offset chosen high enough to energetically separate the  $|2, 2\rangle$  from the  $|2, 1\rangle$  cloud, and then tuning the microwave frequency between the potential minimum seen by  $|2, 1\rangle$  atoms and the untrapped  $|1, 0\rangle$  state [cf. Fig. 1(c)]. Pulse durations of 5 ms have revealed long enough to empty the undesired trapped states. However, this procedure has to be repeated several times during the evaporation process, because the  $|2, 1\rangle$  state is continuously refilled. In contrast the  $|1, -1\rangle$  atoms are removed from the trap once for all at the beginning of the evaporation ramp via irradiation of a microwave swept across the transition to the anti-trapped  $|2, -2\rangle$  state [cf. Fig. 1(d)].

To determine the cross-species scattering length  $a_{\text{mx}}$ , we have measured the thermalization time for sympathetic cooling. Experimentally, we make use of the fact that the thermal equilibrium between the clouds can be disturbed by evaporating the Rb cloud faster than the Li temperature can follow. I.e. we rapidly cool the Rb cloud to a certain temperature and then record the evolution of the Li temperature as a function of time.

The cross-species collision cross section can be extracted from the thermalization speed using the following model [25]. In the case of unequal collision partners about  $2.7/\xi$  collisions per atom are needed for thermalization of a gas,  $\gamma_{\text{thm}} = \xi\gamma_{\text{coll}}/2.7$ . The reduction factor due to the mass difference of the collision partners

is [26]  $\xi = 4m_6m_{87}(m_6 + m_{87})^{-2}$ . The collision rate  $\gamma_{\text{coll}} = \sigma_{\text{mx}}\bar{v}n_{\text{mx}}$  is proportional to the cross section for interspecies collisions,  $\sigma_{\text{mx}} = 4\pi a_{\text{mx}}^2$ , the mean thermal relative velocity  $\bar{v} = \sqrt{(8k_B/\pi)(T_6/m_6 + T_{87}/m_{87})}$ , and the overlap density of the two clouds

$$n_{\text{mx}} \equiv (N_6^{-1} + N_{87}^{-1}) \int n_6(\mathbf{r})n_{87}(\mathbf{r})d^3\mathbf{r}, \quad (1)$$

where  $n_6$  and  $n_{87}$  are the density distributions of the Li and the Rb clouds, respectively. The instantaneous temperature difference  $\Delta T$  evolves according to

$$\frac{d}{dt}(\Delta T) = -\gamma_{\text{thm}}\Delta T. \quad (2)$$

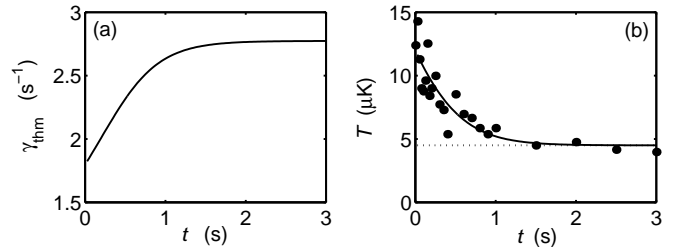


FIG. 3: Measured and simulated evolution of the thermalization process. Both the Rb and the Li clouds are precooled to  $12 \mu\text{K}$ , before the Rb cloud is quickly ramped down to  $5 \mu\text{K}$ . (a) Evolution of the cross-species thermalization rate according to the model Eq. (2). (b) Measured (dots) and calculated (solid line) temperature evolution of the Li cloud. The dotted line indicates the Rb temperature.

Experimentally, we evaporate the Rb cloud to  $12 \mu\text{K}$  within 20 s and wait for the Li cloud to follow up. We then rapidly pursue the evaporation ramp for the Rb cloud down to  $5 \mu\text{K}$  within 300 ms. At that time we find the Li temperature still at  $12 \mu\text{K}$ . The number of Rb atoms is estimated to  $(1.3 \pm 0.6) \times 10^7$ , and the Li atom number is roughly  $10^5$ . Starting with this situation we observe the gradual thermalization of the Li cloud. The microwave radiation is parked at the final frequency of the evaporation ramp, where it skims off those Rb atoms which are heated during the thermalization process. Because of this and because of the larger heat capacity of the bigger Rb cloud, its temperature remains stable, while the Li cloud reduces its temperature until thermal equilibrium with the Rb cloud. Figure 3(b) shows how the temperatures evolve with time. Applying the model outlined above by iterating equation (2), we find that the best fit to the data is compatible with the cross species  $s$ -wave triplet scattering length  $|a_{\text{mx}}| = 17_{-6}^{+9} \text{ a}_\text{B}$ . The small value of the interspecies scattering length explains why the sympathetic cooling dynamics is so slow that it decouples from the forced evaporation process of Rb. Also shown in figure 3(a) is the time-evolution of the calculated cross-species thermalization rate  $\gamma_{\text{thm}}$ . Obviously, it is not constant but increases with time mainly

because the spatial overlap improves as thermalization goes on.

The accuracy of the measurement is limited by the uncertain number of Rb atoms. In contrast, the likewise uncertain Li atom number does not influence the thermalization rate, because for  $N_6 \ll N_{87}$  it drops out of the overlap density (1). Furthermore, since the heat capacity of the clouds depends on the geometry of the trapping potential [27], the number of collisions needed for complete thermalization (about 3 for a harmonic trap) also does. However in radial direction, even at modest temperatures around 10  $\mu\text{K}$ , our potential has linear shape, so that the required number of collisions is expected to be slightly modified (around 4 collisions). And finally, the simple model used to simulate the thermalization dynamics must be taken with care. In fact, it describes the thermalization of two coupled ensembles, each of them being separately in a thermal equilibrium characterized by a distinct temperature. However this assumption does not hold for the Li cloud, which can not equilibrate because of the absence of *s*-wave collisions. These uncertainties are accounted for by a conservative estimation of the error for the scattering length. An improved data analysis would require a complete numerical simulation

of the thermalization dynamics [28].

In conclusion, we have observed sympathetic cooling of a cloud of fermionic lithium by an actively cooled rubidium cloud, although the cross-species thermalization is hindered by two facts: First of all, inelastic collisions with Rb atoms in wrong Zeeman states introduce important losses for the Li cloud, which quickly annihilate the cloud. And second, the very low value for the interspecies scattering length considerably slows down the thermalization process. By repeatedly purifying the Rb cloud and by choosing a slow cooling ramp we could avoid these problems and drive the Li cloud to quantum degeneracy.

A way of manipulating the interspecies scattering length is not only desirable for controlling the thermalization dynamics, but may also prove essential for synthesizing heteronuclear molecules. The scattering length can be efficiently tuned near a Feshbach resonance. A sensible project for the near future could thus be the search for heteronuclear Feshbach resonances. Unfortunately, the long-range behavior of the interatomic potentials for Li-Rb collisions, and hence the location of Feshbach resonances is yet unknown.

We acknowledge financial support from the Deutsche Forschungsgemeinschaft.

---

[1] J. Herbig *et al.*, *Science* **301**, 1510 (2003); C. A. Regal *et al.*, *Nature* **424**, 47 (2003); K. Xu *et al.*, *Phys. Rev. Lett.* **91**, 210402 (2003).

[2] S. Jochim *et al.*, *Science* **302**, 2101 (2003); K. E. Strecker *et al.*, *Phys. Rev. Lett.* **91**, 080406 (2003); J. Cubizolles *et al.*, *Phys. Rev. Lett.* **91**, 240401 (2003); M. W. Zwierlein *et al.*, *Phys. Rev. Lett.* **91**, 250401 (2003).

[3] S. Inouye *et al.*, *Nature* **92**, 08320 (1998); Ph. W. Courteille *et al.*, *Phys. Rev. Lett.* **81**, 69 (1998).

[4] C. Regal *et al.*, *Phys. Rev. Lett.* **92**, 083201 (2004).

[5] D. S. Petrov, *Phys. Rev. Lett.* **93**, 090404 (2004); S.J.J.M.F. Kokkelmans, *Phys. Rev. A* **69**, 031602(R) (2004).

[6] M. Bartenstein, *Phys. Rev. Lett.* **92**, 120401(2004); M. W. Zwierlein *et al.*, *Phys. Rev. Lett.* **92**, 120403 (2004).

[7] J. Voit, *Rep. Prog. Phys.* **57**, 977 (1994); H. Monien, M. Linn, and N. Elstner, *Phys. Rev. A* **58**, 3395 (1998); A. Recati, P. O. Fedichev, W. Zwerger, and P. Zoller, *Phys. Rev. Lett.* **90**, 020401 (2003).

[8] G. Igel-Mann, U. Wedig, P. Fuentealba, and H. Stoll, *J. Chem. Phys.* **84**, 5007 (1986).

[9] M. A. Baranov, M. S. Marénko, V. S. Rychkov, and G. V. Shlyapnikov, *Phys. Rev. A* **66**, 013606 (2002).

[10] L. Santos, G. V. Shlyapnikov, P. Zoller, and M. Lewenstein, *Phys. Rev. Lett.* **85**, 1791 (2000).

[11] C. A. Stan *et al.*, *Phys. Rev. Lett.* **93**, 143001 (2004); S. Inouye *et al.*, *Phys. Rev. Lett.* **93**, 183001 (2004).

[12] A. Fioretti *et al.*, *Phys. Rev. Lett.* **80**, 4402 (1998); A. N. Nikolov *et al.*, *Phys. Rev. Lett.* **82**, 703, (1999).

[13] U. Schlöder, C. Silber, and C. Zimmermann, *Appl. Phys. B* **73**, 801 (2001).

[14] U. Schlöder, C. Silber, T. Deusche, and C. Zimmermann, *Phys. Rev. A* **66**, 061403 (R) (2002).

[15] M. W. Mancini *et al.*, *Phys. Rev. Lett.* **92**, 133203 (2004); A. J. Kerman *et al.*, *Phys. Rev. Lett.* **92**, 153001 (2004).

[16] N. Nygaard and K. Molmer, *Phys. Rev. A* **59**, 2974 (1999); A. P. Albus, F. Illuminati, and M. Wilkens, *Phys. Rev. A* **67**, 063606 (2003); G. Roati, F. Riboli, G. Modugno, and M. Inguscio, *Phys. Rev. Lett.* **89**, 150403 (2002); R. Roth and H. Feldmeier, *Phys. Rev. A* **65**, 021603 (2002).

[17] G. Ferrari *et al.*, *Phys. Rev. Lett.* **89**, 053202 (2002); G. Modugno *et al.*, *Phys. Rev. Lett.* **89**, 190404 (2002).

[18] H. Heiselberg, C. J. Pethick, H. Smith, and L. Viverit, *Phys. Rev. Lett.* **85** 2418 (2000); N. J. Bijlma, B. A. Heringa, and H. Stoof, *Phys. Rev. A* **61**, 053601 (2000); L. Viverit, *Phys. Rev. A* **66**, 023605 (2002).

[19] A. G. Truscott *et al.*, *Science* **291**, 2570 (2001).

[20] F. Schreck *et al.*, *Phys. Rev. Lett.* **87**, 080403 (2001).

[21] H. Ott, J. Fortágh, A. Grossmann, and C. Zimmermann, *Phys. Rev. Lett.* **87**, 230401 (2001).

[22] C. Silber, PhD thesis, Tübingen (2005) unpublished.

[23] Z. Hadzibabic *et al.*, *Phys. Rev. Lett.* **88**, 160401 (2002).

[24] C. J. Myatt *et al.*, *Phys. Rev. Lett.* **78**, 586 (1997); F. H. Mies, C. J. Williams, P. S. Julienne, and M. Krauss, *J. Res. Natl. Inst. Stand. Tech.* **101**, 521 (1996).

[25] G. Delannoy *et al.*, *Phys. Rev. A* **63**, 051602 (2001).

[26] M. Mudrich *et al.*, *Phys. Rev. Lett.* **88**, 253001 (2002);

[27] O. J. Luiten, M. W. Reynolds, and J. T. M. Walraven, *Phys. Rev. A* **53**, 381 (1996).

[28] Huang Wu and Ch. J. Foot, *J. Phys. B* **29**, L321 (1996).